J Fluoresc (2011) 21:753–763
DOI 10.1007/s10895-010-0766-2

ORIGINAL PAPER

Conformational Transitions in *Ariesaema curvatum* Lectin: Characterization of an Acid Induced Active Molten Globule

Urvashi Sharma · Sushama M. Gaikwad · C. G. Suresh · Vikram Dhuna · Jatinder Singh · Sukhdev Singh Kamboj

Received: 16 August 2010 / Accepted: 25 October 2010 / Published online: 11 November 2010

Abstract Biophysical characterization of a lectin from *Ariesaema curvatum* (ACL) was carried out using steady state as well as time resolved fluorescence and CD spectroscopy under various denaturing conditions. An intermediate with altered tryptophan microenvironment was detected in the phase diagram, which exibited pronounced secondary structure and hemagglutinating activity in presence of 0.25 M Gdn–HCl. An acid induced molten- globule like structure possessing activity and higher thermostability was detected. Transition to the molten globule state was reversible in nature. The lectin retained hemagglutinating activity even after incubation at 95 °C. Both chemical and thermal unfolding of the lectin were found to consist of multistate processes. Fluorescence quenching of ACL was strong with acrylamide and KI. The single tryptophan was found to be surrounded by high density of the positively charged amino acid residues as shown by a ten fold higher K_{sv} for KI compared to that for CsCl. The average lifetime of tryptophan fluorescence increased from 1.24 ns in the native state to 1.72 ns in the denatured state.

U. Sharma · S. M. Gaikwad (✉) · C. G. Suresh
Division of Biochemical Sciences, National Chemical Laboratory, Pune, Maharashtra 411008, India
e-mail: sm.gaikwad@ncl.res.in

V. Dhuna · J. Singh · S. S. Kamboj
Department of Molecular Biology and Biochemistry, Guru Nanak Dev University, Amritsar 143005 Punjab, India

Keywords Molten globule · Unfolding · Thermostability · Secondary structure · Fluorescence lifetime · Araceae · Hemagglutinin

Introduction

Molecular recognition of carbohydrates by proteins is of prime importance in many biological processes, such as viral, bacterial, mycoplasmal and parasitic infections, targeting of cells and soluble components, fertilization, cancer metastasis and growth and differentiation. Lectins are the carbohydrate binding proteins of non-immune origin which have got ubiquitous occurrence in nature ranging from microorganisms to plants, insects and animals and have been found to evoke variety of biological responses simply by binding to their cognate carbohydrate ligands. Agglutination is the most easily detectable evidence of the interaction of lectin with cells due to their multivalency. Plant lectins possess one or more non-catalytic domains that bind reversibly to specific sugar structures and mediate a variety of biological processes, such as cell-cell and host-pathogen interactions, serum glycoprotein turnover and innate immune responses [1]. The crystal structures of the lectin-carbohydrate complexes turn out to be excellent model systems to study protein-carbohydrate interactions.

In addition, plant lectins showing specificity for complex sugar where the hemagglutination is inhibited only by complex glycoproteins and not by simple sugars have also been reported. The examples are *Scilla campanulata* bulb lectin [2], *Acacia constricta* seed lectins [3], *Arisaema*

flavum tuber lectin [4]. However, the structures of these lectins are not well characterized except for that of a lectin from *Scilla campanulata* (SCAfet) specific for complex glycoproteins is reported (PDB code 1dlp) [5]. Studies on lectins showing specificity for complex sugars are fewer and there is a need to characterize them in detail to understand their biochemical properties and differences contributing towards the sugar recognition.

Lectins are reported to be abundant in araceae family constituting 70–80% of the tuber storage proteins [6]. Araceace lectins are classified under the superfamily of monocot mannose binding lectins according to their sequence homology and sugar specificity [7]. Other members of Man-binding lectins from Amaryllidaceae [8], Alliaceae [8], and Orchidaceae [9] family are well studied. However, compared to these, the lectins from araceae are found to interact strongly towards the glycoproteins. Though grouped into the mannose binding lectin family, non-mannose binding monocot lectins which are showing specificity for complex sugars are purified and characterized from the tubers of the different araceous plants e.g *Sauromatum guttatum Schott* (SGA), *Arisaema curvatum Kunth* (ACmA), *Arisaema tortuosum schott* (ATL), *Gonatanthus pumilus* (GPL) [10] and *Alocasia indica* (AIL) [11].

We have reported structure-activity relationship of few of the plant lectins which are involved in the recognition of complex sugars like *Cicer arietinum* lectin (CAL) and *Moringa oleifera* lectin (MoL) [12, 13]. Dharkar et al. 2009 [14] had reported biophysical characterization of two Araceae lectins involved in recognition of complex sugars. In this communication we are reporting the biophysical characterization of Araceae lectin from *Arieaema curvatum* (ACL) showing specificity for complex sugars.

ACL, a 13 KDa protein isolated from the tubers of *Ariesaema curvatum* was found to possess mitogenic potential for human blood lymphocytes [10] and exists as a mixture of isolectins differing in charge similar to the *Alocasia indica* lectin [11]. Our studies are an attempt to characterize the araceae lectin ACL, showing specificity for complex sugars. We also show for the first time an acid induced molten globule of ACL in the reversibly active form which could be one of the intermediate during protein folding pathway.

Experimental

Materials

ACL was purified according to the method described earlier [10]. Potassium dihydrogen monophosphate, dipotassium hydrogen phosphate, sodium chloride, citric acid were purchased from Merck, India. Guanidium hydrochloride (GdnHCl), 8-Anilino-1-naphthalene sulfonic acid (ANS), N-bromosuccinimide, were purchased from Sigma, USA.

Methods

Hemagglutination Assay

Rabbit RBCs were washed 5 times with PBS (phosphate buffer saline, 10 mM potassium phosphate buffer pH 7.2 containing 150 mM NaCl). A 3% (v/v) suspension of the erythrocytes in the same buffer was prepared. Hemagglutination assays were performed according to Gurjar et al. 1998 [15].

Circular Dichroism Spectroscopy

CD spectra of ACL samples were recorded at room temperature using a Jasco J-815-150S (Jasco, Tokyo, Japan) spectropolarimeter connected to a Peltier Type CD/FL Cell circulating water bath. For far UV analysis the spectra were recorded in the range of wavelengths 200–250 nm at a scan speed of 100 nm min-1 with a response time of 1 s and slit width 1 nm. A rectangular quartz cell of 1 mm path length was used. The lectin concentration used was 0.1 mg ml^{-1} for all the samples. Each spectrum was obtained as an average of 5 scanned ones.

To study the effect of pH on the secondary structure of ACL, the following buffers were used: 20 mM Glycine–HCl (pH 1.0–3.0), 20 mM citrate-phosphate (pH 4.0–5.0), 20 mM phosphate (pH 6.0–7.0), 20 mM Tris–HCl (pH 8.0–9.0), and 20 mM glycine/NaOH (pH 10.0–12.0). Protein samples were incubated for 5 hrs against the buffer of appropriate pH before recording the spectra.

To monitor the effect of chemical denaturation of the ACL, the protein was incubated in GdnHCl in the concentration range of 0–6 M at pH 7.0 and 0–4 M at pH 3 for 5 hrs. Buffer scans recorded under the same conditions were subtracted from the lectin spectra for further analysis.

To study the tertiary structure of the ACL at pH 3.0 and 7.0, the near-UV CD spectra were recorded in the range of 250–300 nm using a cuvette of path length 1 cm. The lectin concentration used was 1 mg/ml.

The effect of temperature on the secondary structure of ACL was studied at pH 7.0 and 3.0 by increasing the temperature of the protein samples at the rate of 2 °C/min in the temperature range 25–95 °C. The interval of 10 °C was used and the ellipticity was recorded between 200–250 nm. All data were corrected for respective buffer base line.

Steady State Fluorescence Spectroscopy

Intrinsic fluorescence of the protein was measured using a Perkin Elmer LS50 fluorescence spectrophotometer. The

samples were kept in a quartz cuvette, at room temperature. The background emission due to the signal produced by either buffer solution, or buffer containing the appropriate quantity of denaturants was subtracted. The lectin solution (~0.05 mg ml^{-1}) was excited at 280 as well as at 295 nm and the emission spectra were recorded between 300–400 nm. Both the excitation and emission spectra were obtained setting the slit-width at 7 nm, and speed 100 nm min^{-1}. To see the effect of pH on fluorescence maximum, ACL was incubated at different pH ranges from 1–12 in the respective buffers for 5 hrs. Before analysis the respective buffer spectra were subtracted from the protein spectra.

Steady-state Fluorescence Quenching of ACL

Fluorescence quenching measurements were performed for native (at pH 7.0) and protein incubated at pH 3.0 with different quenchers like acrylamide (5 M), iodide (5 M) and cesium ions (5 M) by titrating the protein sample (0.05 mg/ml) prepared in 20 mM phosphate buffer, pH 7.0 against small amounts of quencher stock solutions. Sodium thiosulfate (0.2 M) was added to the iodide stock solution to prevent the formation of tri-iodide (I3). Relative fluorescence intensities were measured at the

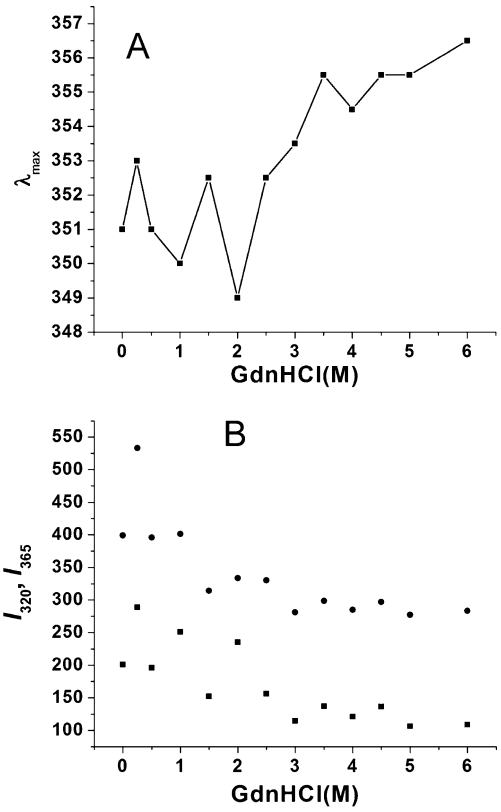

Fig. 1 GdnHCl induced unfolding of ACL. **a** Shift in λmax of unfolded ACL vs GdnHCl concentration. **b** Change in tryptophan fluorescence at 320 (filled square) and 365 nm (filled circle) with increasing concentration of GdnHCl. All Protein (0.05 mg ml^{-1}) incubations were done in 20 mM phosphate buffer, pH 7.0 containing required GdnHCl concentration for 5 h at 25 °C

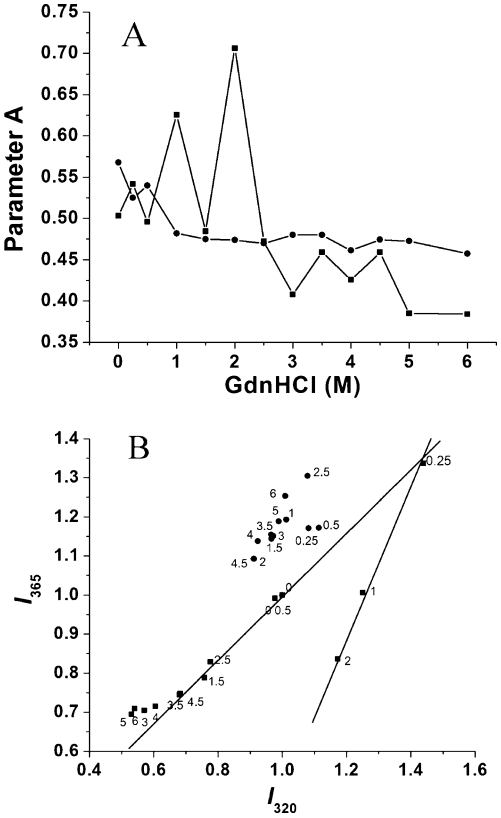

Fig. 2 Parameter A (**a**) and Phase diagram (**b**) of ACL treated with GdnHCl. The parameter A was plotted as the ratio of intrinsic fluorescence intensity at 320 nm (I_{320}) to that of 365 nm (I_{365}). Phase diagram was constructed by monitoring the changes of I_{365} as a function of I_{320}. (Filled squares and filled circles represent unfolding and refolding respectively)

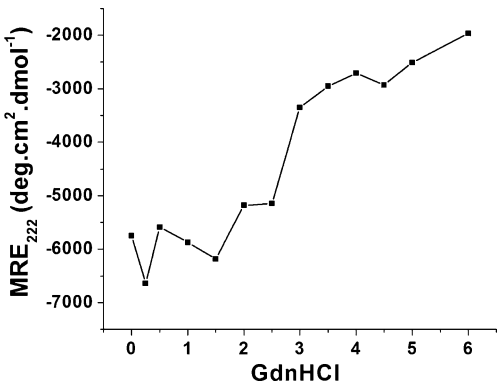

Fig. 3 Effect of GdnHCl on MRE at 222 nm. The ellipticity values were taken from the far UV CD spectra of GdnHCl treated protein (0.1 mg ml^{-1}). The samples were incubated for 5 h at 25 °C

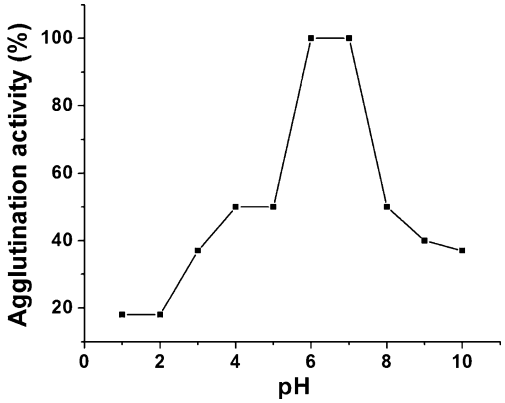

Fig. 4 Effect of pH on Hemagglutination activity of ACL. The assay was carried out as described in "Materials" and "Methods". The samples (14 μg) were incubated in the buffers of respective pH for 5 h

wavelength corresponding to the emission maximum (351 nm) of the protein and volume correction for fluorescence intensities was done before analyzing the quenching data [16].

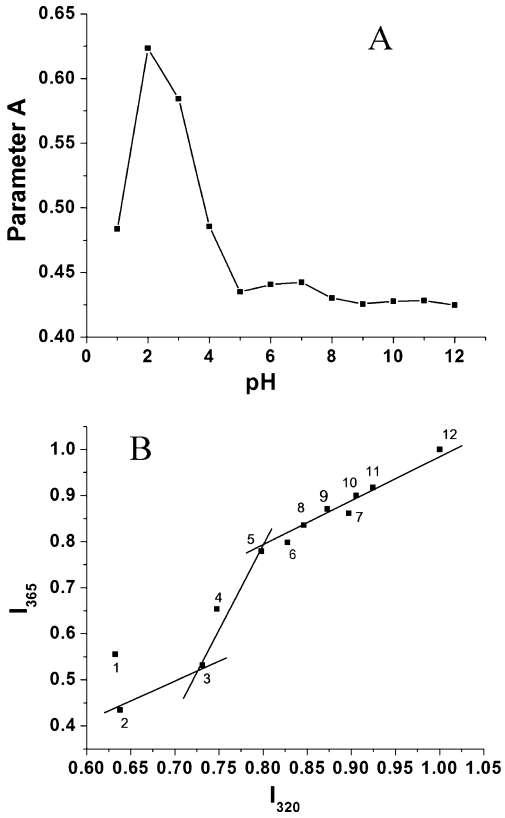

Fig. 5 Parameter A (**a**) and Phase diagram (**b**) of ACL as a function pH. The parameter A was plotted as the ratio of intrinsic fluorescence intensity at 320 nm (I_{320}) to that of 365 nm (I_{365}). Phase diagram was constructed by monitoring the changes of I_{365} as a function of I_{320}. The lectin concentration used was 0.05 mg ml^{-1} and the samples were incubated in the buffers of respective pH for 5 h at 25 °C

Fluorescence Lifetime Measurement

Lifetime fluorescence measurements were carried out by employing CW-passively mode-locked frequency-doubled Nd: YAG laser (Vanguard, Spectra Physics, USA)- driven rhodamine 6 G dye laser which generates pulses of width ~1 ps. Fluorescence decay curves were obtained by using a time-correlated single-photon counting set up, coupled to a microchannel plate photomultiplier (model 2809u; Hamamatsu Corp.). The instrument response function (IRF) was obtained at 295 nm using a colloidal suspension of dried non-dairy coffee whitener. The samples were excited at 295 nm and the fluorescence emission was recorded at 353 nm. The slit width of emission monochromator was 7 nm. The resultant decay curve was analyzed by a multi-exponential iterative fitting program provided with the instrument. Concentration of ACL samples were 0.3 mg/ml for the experiments.

Binding of Hydrophobic dye ANS to ACL

The binding of the hydrophobic dye 8-Anilino-1-naphthalene sulfonic acid (ANS) was studied by recording the emission spectra in the range 430–550 nm with excitation

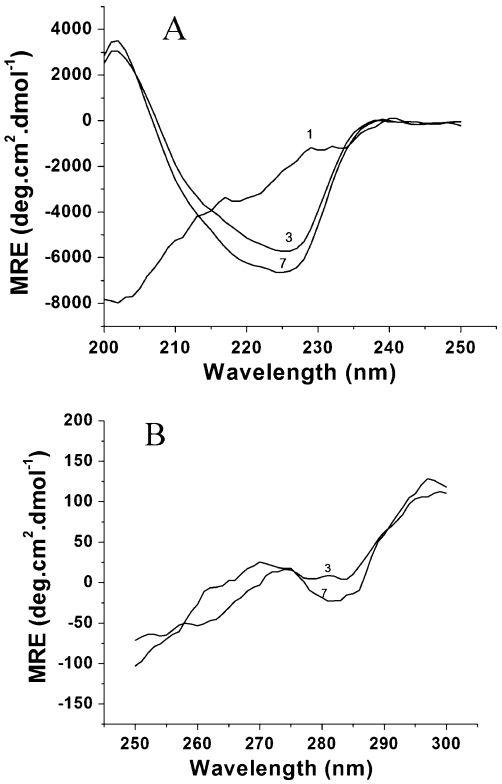

Fig. 6 Effect of pH on the structure of ACL. Far-UV (protein concentration 0.1 mg ml^{-1}) (**a**) and Near-UV (1 mg ml^{-1}) (**b**) CD spectra of ACL at native and acidic pH (The numbers on the spectra correspond to the pH of the protein.) All the pH incubations were carried out in the respective buffers for 5 h at 25 °C

Table 1 Secondary structure analysis of ACL as a function of pH, temperature and chemical denaturants. The far-UV CD spectra of the ACL under these conditions were analyzed by CDSSTR programme available online with CDPRO suit

ACL	Helix	Sheet	Turn	Unordered	NRMSD
Native	4.9	45.2	18	31.4	0.07
pH 3.0	5.5	39.5	23.3	31.3	0.08
4 M Gdn–HCl (pH 7)	5.5	34.5	33.6	26.4	0.07
95 °C (ph 7)	5.3	36.3	25.2	31.0	0.09
Recooled at 25 °C (pH 7)	5.2	40.2	23.2	30.5	0.06

at 375 nm using steady-state spectrofluorimeter. The protein was incubated at different pH in the range from 1–12 in the respective buffers. 5 μl of 15 mM ANS was mixed with 2 ml of protein (0.03 mg/ml). Buffer spectrum with ANS in each of the condition was subtracted from the spectrum of the protein.

Phase Diagram and Parameter A Analysis

Parameter A is the ratio of fluorescence intensity at 320 nm to that at 365 nm of the steady state fluorescence is the characteristic of the shape and position of fluorescence spectra [17]. Parameter A is used for monitoring protein conformational changes [18, 19]. Phase diagram analysis was also carried out for ACL to detect the folding intermediates. To construct the phase diagram the fluorescence intensity at 320 nm versus 365 nm at different GdnHCl concentrations as well as at varying pH was analysed as described previously [18, 20]. The data were normalized by the corresponding intensity of the spectra for native protein. In the phase diagram the straight line represents an all-or-none process, while the non-linearity between I_{320} and I_{365} reflects that the structural transition involves folding intermediate(s). The crossover of the two lines corresponds to the appearance of intermediate at that pH/ GdnHCl concentration.

Results and Discussion

Chemical Denaturation of ACL

The intrinsic fluorescence spectrum of ACL, a single tryptophan protein, shows the emission maximum at

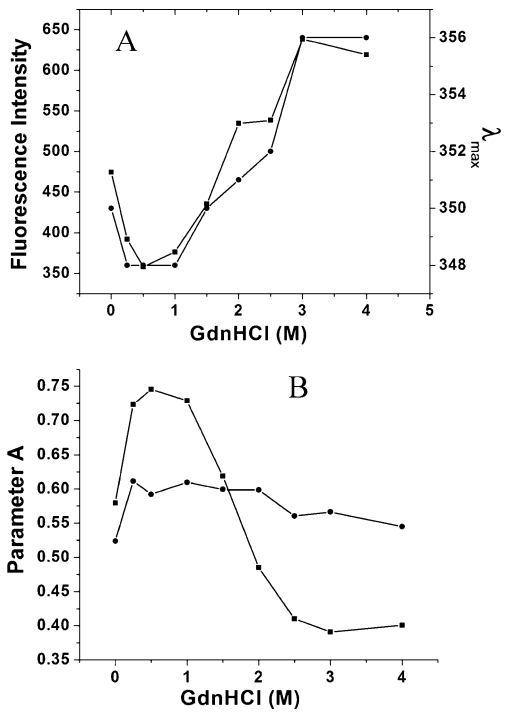

Fig. 7 Characterization of the acid-induced molten globule state of ACL. Effect of GdnHCl on fluorescence intensity (filled square) and λmax (filled circle) of the protein (0.04 mg ml^{-1}) at pH 3.0 (**a**), Parameter A at pH 3.0 (**b**) (filled square and filled circle represents unfolding and refolding respectively.)

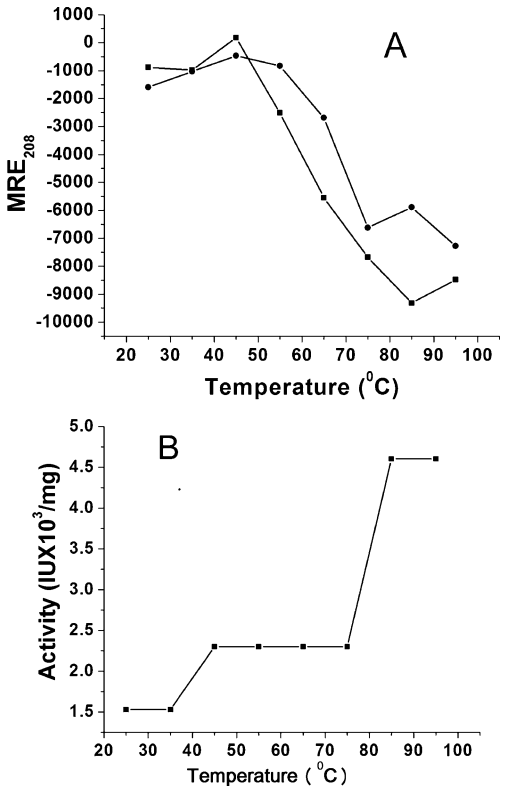

Fig. 8 Thermal unfolding of ACL (0.1 mg ml^{-1}) at pH 7.0 and pH 3.0. MRE $_{208}$ as a function of temperature (filled square and filled circle for native and pH 3.0 incubated ACL respectively) (**a**) and hemagglutination activity as a function of temperature (**b**)

351 nm indicating the tryptophan residue to be exposed to the solvent. The shift in the λmax and change in the fluorescence intensity of ACL with increasing concentration of GdnHCl are shown in Fig. 1a and b, respectively. The perturbation in the tryptophan environment of ACL in presence of 0.25–2.5 M GdnHCl was reflected in the alternate red and blue shift in the λmax of fluorescence emission (Fig. 1a). In presence of 0.25 M GdnHCl, fluorescence intensity at 365 nm increased 1.5 times while at 0.5 M it decreased to the original level (Fig. 1b) indicating the alteration in the micro-environment of the tryptophan due to breakage of weak interactions resulting in enhanced and reduced fluorescence emission. Significant perturbation in the fluorescence intensity at 320 nm, up to 2 M GdnHCl indicated alteration in the micro-environment of hydrophobic conformer of the tryptophan. At 3 M GdnHCl and above the fluorescence intensity remained stable. Gradual red shift in the λmax was observed which reached up to 356 nm with 34% decrease in the fluorescence intensity in presence of 6 M GdnHCl indicating exposure of tryptophan to more polar environment due to unfolding of the protein.

Parameter A (ratio of *I*320 and *I*365) gives the idea about shape and position of the tryptophan spectrum and the phase diagram plotted as the *I*320 vs *I*365 gives the information regarding intermediates existing during unfolding. Parameter A for ACL shows the formation of several intermediates of protein in the presence of 0.25–2.5 M GdnHCl (Fig. 2a). However, after renaturation, refolding of the protein seems to be quite in order. Two linear portions were observed in the phase diagram for unfolding of ACL (Fig. 2b). The two lines intersect at 0.25 M GdnHCl indicating the presence of an intermediate. The intermediate was able to retain complete hemagglutination activity as that of native lectin. No linearity was observed in the phase diagram of the refolding of ACL.

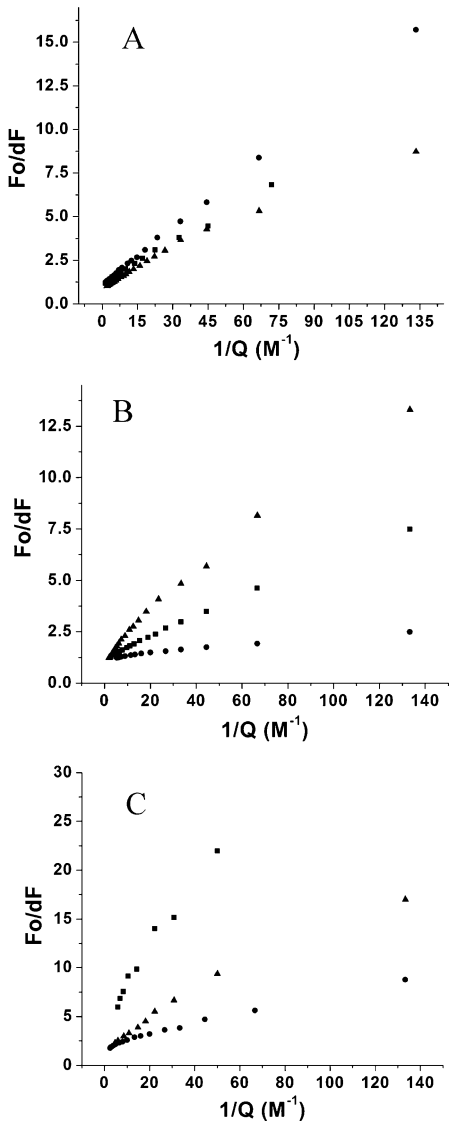

Fig. 9 Fluorescence quenching analysis of ACL. Modified Stern-Volmer plots for acrylamide (**a**), KI (**b**) and CsCl (C) as the quenchers for the native (filled square), 6 M Gdn–HCl denatured (filled triangle) and ACL at pH 3.0 (filled circle). After fitting the data the R value in each case was 0.99.The titrations of ACL (0.05 mg ml^{-1}) with different quenchers were carried out as described in the section of "Materials" and "Methods"

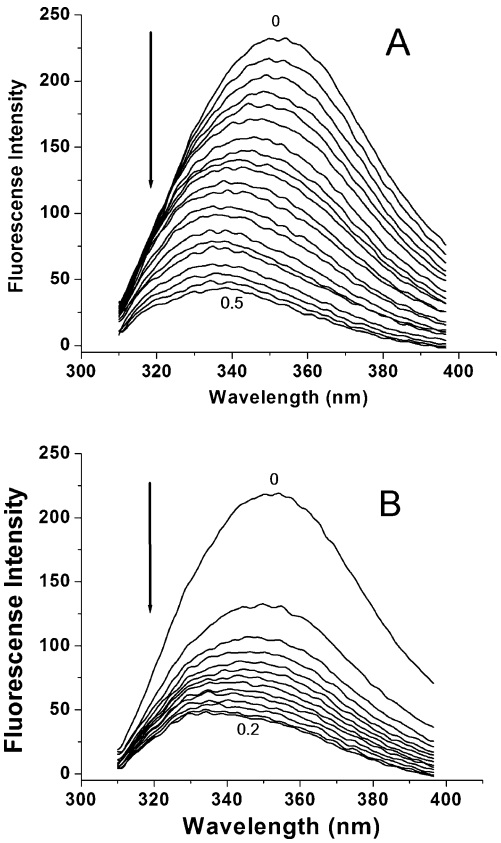

Fig. 10 Fluorescence spectra of ACL (0.05 mg ml^{-1}) quenched with acrylamide (**a**) and KI (**b**) at pH 3.0

Far-UV CD spectra for ACL treated with different concentrations of GdnHCl were recorded. At 0.25 M GdnHCl, the decrease in the negative ellipticity (Fig. 3) indicated more pronounced secondary structure confirming the existence of an intermediate. Major transition in the secondary structure of the protein was observed between 2.5 and 3.0 M GdnHCl. Above 3 M GdnHCl, the negative ellipticity decreased slowly. Maximum unfolding took place at 6 M GdnHCl. The existence of an intermediate species between 2.0–2.5 coincides with that observed in the plot of I_{365} vs. concentration of GdnHCl (Fig. 1b). Thus, both the fluorescence and CD data reveal the multistate unfolding of ACL in the presence of GdnHCl. The anomalous behavior of ACL in presence of 0.25 to 2.5 M GdnHCl i.e. instantaneous changes in the tryptophan microenvironment (alternate increase and decrease in the fluorescence intensity and red and blue shift in the λ max) and secondary structure (increase and decrease in the negative ellipticity) is an interesting feature of ACL.

Effect of pH on the Structure and Stability of ACL

ACL samples were checked for activity in appropriate buffers in the pH range 1–10, by hemagglutination assay and the residual activities observed were plotted as a function of pH (Fig. 4). The lectin showed maximum activity at pH 6–7 while it declined towards both acidic and alkaline pH. ACL was found to be active in wide pH range for 5 hrs. Very few plant lectins are known to be stable in such a wide range of pH, some of them are: lectin from Pinto beans (pH range: 3–12) [21]; *Alocasia cucullata* lectin (pH range: 2–12) [22] and *Arisaema tortuosum* lectin (pH range: 2–10) [23].

At pH 2.0 twofold decrease in the fluorescence intensity of the protein at 365 nm was observed. This could be due to the quenching of fluorescence due to protonation of amino acids around tryptophan. Tryptophan in ACL at pH 3 is probed into relatively hydrophobic environment as revealed by the blue shift of 3 nm in λmax (data not shown).

The parameter A (Fig. 5a) and phase diagram (Fig. 5b) for pH-fluorescence profile were plotted. Parameter A shows the transition in the structure of the protein between pH 4.0–2.0 and again from 2.0-1.0. The phase diagram shows the existence of two stable intermediates at pH 3.0 and pH 5.0. The intermediate at pH 3.0 was taken up for further characterization. The intermediate at pH 5.0 could be formed due to no net charge on the protein (pI).

In the far UV CD spectrum of native ACL, sharp minima around 225 nm and positive maxima at 205 nm was observed (Fig. 6a). The secondary structure prediction by CDSSTR program from CDPro showed α-helix: 4.9%, β-sheet: 45%, turns: 18% and random coil: 31%. Thus ACL is a beta protein containing frequent turns and unordered elements. The negative minima at 225 nm and maxima around 200 nm is well characterized for type III β turns in the case of tuftsin a synthetic tetrapeptide [24]. This could be due to high content of proline-glycine repeats in ACL as reported by Brahmachari et al. 1982 [25] in case of trypeptides with pro-gly sequences. Our observation suggests that this type III β turns seems to be conserved pattern in araceae lectins, well characterized in case of lectins from *Arisaema tortuosum* (ATL) and *Sauromatum guttatum* Schott (SGA) [14].

At pH 1, complete loss of secondary structure and at pH 3, 20% loss in the secondary structure was seen in far-UV CD spectra of ACL (Fig. 6a). The protein is able to retain the major structure at pH 3.0.

ANS binding studies of ACL were carried out to study the unfolding intermediates of the protein. ACL at pH 7, alkaline pH and at pH 4–6 failed to bind ANS while

Table 2 Summary of parameters obtained from Stern–Volmer and modified Stern–Volmer analysis of the intrinsic fluorescence quenching of ACL with different quenchers

Quencher and Samples	$K_{sv1}(M^{-1})$	k_{q1} ($\times 10^9$ M^{-1} S^{-1})	$K_{sv2}(M^{-1})$	k_{q2}($\times 10^9$ M^{-1} S^{-1})	f_a	$K_a(M^{-1})$
Acrylamide						
Native	7.5	6.04	–	–	0.86	16.6
pH 3.0	9.0	–	–	–	0.93	10.7
6 M Gdn–HCl	–	–	–	–	0.91	18.2
KI						
Native	10.9	8.8	16	12.90	0.77	–
pH 3.0	23.6	–	14.7	–	0.83	–
6 M Gdn–HCl	8.3	4.8	–	–	0.73	15.2
CsCl						
Native	1.02	0.8	–	–	0.19	16.3
pH 3.0	2.44	–	–	–	0.46	–
6 M Gdn–HCl	1.6	0.95	–	–	0.62	10.8

maximum binding was observed at pH 1.0 with 5-fold increase in the fluorescence intensity and blue shift in the λmax from 520 to 489 nm indicating fully exposed hydrophobic amino acids on the surface (data not shown). Significant ANS binding was observed at pH 3.0 with 3 times increase in the fluorescence intensity and a blue shift in wavelength maximum from 520 to 495 nm. Thus, the comparatively compact structure of ACL at pH 3 with hydrophobic amino acid side chains exposed on the surface indicates the existence of the lectin in molten globule like structure. This was further confirmed by the near-UV CD spectra where reduced tertiary structure of the protein at pH 3 was observed (Fig. 6b).

Characterization of the Molten Globule of ACL

This acid induced molten globule form of ACL was found to have rearranged secondary structure (1.5% increase in helical content, 5% more turns and 6% loss of beta sheet as listed in Table 1). The geometry at sugar binding site of the lectin remains intact as the protein retained 40% of the hemagglutination activity even after incubation at pH 3.0. This observation suggests the role of this acid induced molten globule to be involved in the late stages of protein folding.

Unfolding of ACL Molten Globule

Decrease in the fluorescence intensity and blue shift in the λmax of ACL in presence of GdnHCl up to 1.0 M concentration at pH 3.0 was observed (Fig. 7a). Increase in the fluorescence intensity and red shift in the λmax was observed at and above 1.5 M GdnHCl, the trend opposite to that observed at pH 7.0 (Fig. 1a and b). The amino acid side chains in the microenvironment of tryptophan are protonated due to which the fluorescence is quenched at pH 3.0 and it still gets quenched at lower concentration of GdnHCl. Thus the conformation of the intermediate at pH 3.0 is significantly different than the native or the unfolded one. The parameter A shows the presence of a stable intermediate between 0.5–1.0 M GdnHCl concentration (Fig. 7b). The renaturation almost refolded the protein to the original protein like state (at pH 3.0).

Thermal Stability of ACL Molten Globule

Thermal denaturation of ACL at pH 7.0 and pH 3.0 as studied by far-UV CD seems to be a multistate process. The secondary structure of ACL at pH 7.0 remained intact at temperature up to 45 °C while at pH 3.0 it was stable up to 55 °C as monitored by MRE 208 (Fig. 8a). The loss of structure at 65 °C was less at pH 3.0 than at pH 7.0. This evidence supports the existence of rigid and compact molten globule state of ACL at pH 3.0 showing the strong intra molecular interaction between the side chains of the protein.

The CD analysis showed that the thermal unfolding at pH 7.0 was reversible and ACL was able to refold back to the native conformation as seen in the secondary structure elements (Table 1). This was in agreement with the hemagglutination assay which showed progressive increase

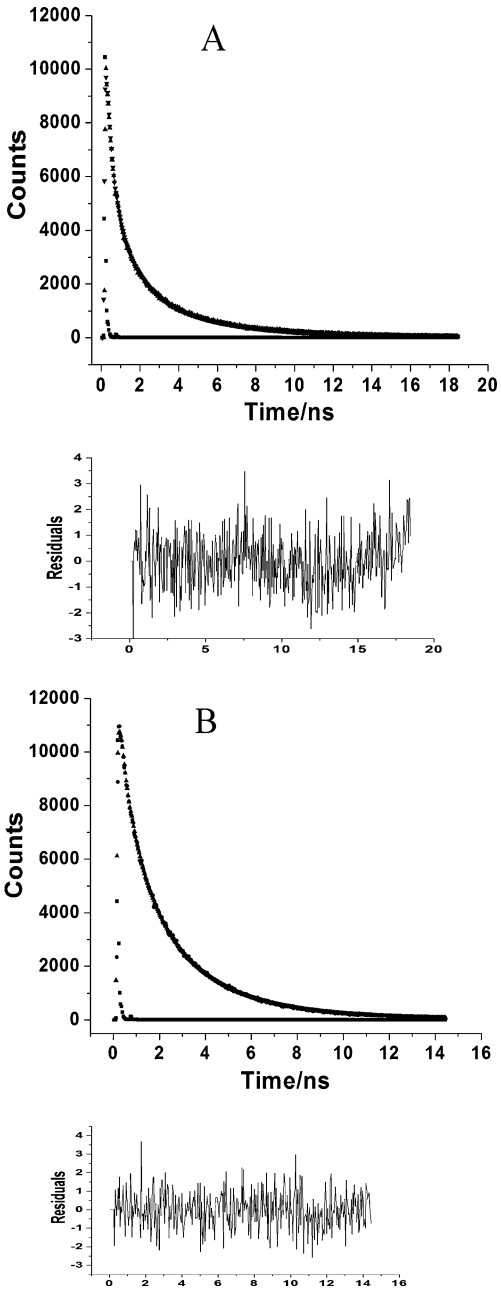

Fig. 11 Life time measurement of ACL. Time resolved fluorescence decay profile of native ACL (0.3 mg ml^{-1}) (**a**) and 6 M GdnHCl denatured (**b**). The solid line corresponds to the nonlinear least square fit of the exponential data. The lower panel represents the residual

in the activity with increase in temperature showing activity maximum for the sample heated at 95 °C (Fig. 8b). The intact and stable active site structure was resumed upon cooling, possibly due to the small energy barrier required for the thermal unfolding. While at pH 3 once incubated at 95 °C, ACL remained in the unfolded state even after cooling back to 25 °C (data not shown).

Fluorescence Quenching Studies on ACL

Solute quenching studies were carried out to study the microenvironment of tryptophan as the protein was found to lose the hemagglutinating activity on modification of the residue. Also, as a part of characterization of the molten globule, the quenching studies of ACL were carried out at pH 3.0. Analysis of the quenching data was performed using the Stern–Volmer and modified Stern–Volmer equations [26]. Modified Stern–Volmer plots for quenching with the various quenchers under native, at pH 3 and for denatured protein are shown in Fig. 9.

Fluorescence quenching efficiency of ACL was highest with iodide. Stern–Volmer analysis for iodide showed downward curvature of the plot, which could be resolved into two linear components (data not shown) suggesting more than one population of tryptophan in the protein, one getting quenched before the other. The K_{sv} value for acrylamide is 7.5 M^{-1} while that for I^- is 10.94 M^{-1} (K_{sv1}) and 12.92 M^{-1} (K_{sv2}). The higher value of K_{sv} for Iodide than that of acrylamide is unusual. Very low K_{sv} for CsCl indicated high density of positive charge around surface tryptophan. The modified Stern-Volmer analysis showed slight increase in the accessibility for acrylamide while the accessibility for I^- decreased slightly after denaturation of the protein. The higher K_{sv} and lower accessibility for I^- as compared to acrylamide could be due to the capacity of the later to penetrate into the interior of the protein.

The profile obtained from Stern-Volmer analysis with acrylamide quenching showed a positive curvature at pH 3 which indicated presence of both dynamic and static quenching components. The static mechanism involves complex formation, while dynamic mechanism involves collisions with acrylamide during the lifetime of tryptophan in excited state.

Accessibility of the fluorescence to CsCl was 19% in the native state, 62% in the denatured state and 46% at pH 3.0 suggesting that the protein is in different conformational state at pH 3.0 and the negative charge density on the surface is significantly increased.

At pH 3 both acrylamide and KI exhibited enchanced quenching associated with a blue shift of 14 nm revealing that after quenching the fluorescence of surface tryptophan conformer, the protein shows fluorescence from conformer in the hydrophobic interior (Fig. 10). Significant loss in the native conformation of ACL and major change in the side chain arrangement of aromatic residues was observed.

Iodide having a large ionic radius and being negatively charged, probably binds to the positively charged amino acid residues of ACL on the surface at pH 3.0 which is reflected in 83% accessibility to the fluorescence. The K_{sv} further increased at pH 3.0 (Table 2). There could also be a possibility of some nonspecific binding of iodide to the protein around the single tryptophan in the protein leading to affinity quenching of the fluorescence rather than collisional quenching.

The lifetime measurement of the intrinsic fluorescence of ACL from the decay curve (Fig. 11) was carried out by fitting it to a multiexponential function (χ^2=1.095). The decay curve of native lectin consists of three components with the lifetimes, τ1 (0.28 ns) and τ2 (1.14 ns) and τ3 (4.11 ns). This indicates the presence of three conformers of the single tryptophan with average lifetime of 1.24 ns (Fig. 11) (Table 3). The ACL denatured with 6 M Gdn–HCl showed increased average life time of 1.72 with τ1 (0.31 ns) and τ2 (1.18 ns) and τ3 (3.11 ns) due to change in the environment of tryptophan after unfolding of protein.

The decay curve of the life time measurements of ACL quenched with 0.5 M acrylamide revealed existence of four

Table 3 Parameters obtained from lifetime fluorescence spectroscopy of ACL (Values in the parentheses indicate amplitudes)

Samples	τ 1 (ns)	τ 2 (ns)	τ 3 (ns)	τ 4 (ns)	<τ> (ns)	χ^2
Native	0.28 (0.49)	1.14 (0.33)	4.11 (0.17)	–	1.24	1.095
Native +0.5 M Acrylamide	0.04 (0.33)	0.23 (0.41)	0.83 (0.18)	1.77 (0.06)	0.38	1.147
Native +0.5 M KI	0.06 (0.29)	0.27 (0.32)	0.74 (0.34)	2.28 (0.03)	0.44	1.123
Native +0.5 M CsCl	0.14 (0.37)	0.52 (0.34)	1.96 (0.18)	4.51 (0.1)	1.03	1.041
Denatured 6 M GdnHCl	0.31 (0.25)	1.18 (0.35)	3.11 (0.39)	–	1.72	1.004
Denatured +0.5 M Acrylamide	0.19 (0.37)	0.53 (0.53)	1.29 (0.09)	–	0.47	1.026
Denatured +0.5 M KI	0.19 (0.26)	0.48 (0.22)	0.94 (0.40)	1.72 (0.10)	0.73	1.198
Denatured +0.5 M CsCl	0.22 (0.24)	1.12 (0.45)	2.50 (0.30)	–	1.32	1.046

conformers of tryptophan. Four times decrease in τ1 (0.04 ns) and τ2 (0.23 ns) and τ3 (0.83 ns) was observed. τ1, τ2, τ3 and the fourth conformer of τ4 (1.77 ns) showed average τ of 0.38 ns (Table 3).

Similar effect was observed in the decay curve upon quenching with KI where τ4 was detected and the average life time was calculated as 0.44 ns. Although in steady state fluorescence quenching, K_{sv} for iodide was greater than that for acrylamide, time resolved measurement gave higher average lifetime for iodide quenched ACL than that for acrylamide quenched protein (0.38 ns). This could be due to some non-specific binding of iodide with the protein due to the higher density of positive charge around surface tryptophan. The tryptophan lifetime was found to be longest for the Cs^{+} quenched protein with average τ of 1.03 ns and 1.32 ns in the native and denatured state, respectively.

In conclusion, our studies on ACL reveal that the tryptophan microenvironment gets perturbed at low concentration of the chemical denaturant. There exists an active intermediate at 0.25 M GdnHCl with altered tryptophan microenvironment and pronounced secondary structure. At pH 3 the protein shows compact secondary and slightly disrupted tertiary structure with hydrophobic amino acid side chains exposed on the surface. This alternative conformation of ACL, identified as a molten globule was able to retain the hemagglutination activity suggesting that the architecture of the sugar binding site either remains intact or can regain the original geometry. Molten globule states have been characterized increasingly in past decade for the diverse range of proteins including lectins; however, to the best of our knowledge only Peanut lectin in its molten globule state has been reported to retain the carbohydrate binding capacity [27]. The structure of ACL molten globule could be considered to be highly ordered one occurring late during the stages of protein folding as reported for IL-4 [28]. Thermal unfolding studies revealed the acid induced molten globule to be rigid in nature while the chemical denaturation profile was significantly different than that at pH 7.0. ACL at pH 3.0 resumes the native structure upon titration to pH 7.0 as observed in the CD profile (data not shown) indicating the reversible transition of the native to the molten globule state. The pH dependent unfolding of ACL can be explained as a three state process such as N ⇔ MG⇒U. This will further pave the way for understanding the protein folding mechanism in the lectins showing specificity for complex sugars.

Acknowledgments The authors wish to thank Dr. Arvind Sahu, NCCS, Pune, and Prof. G. Krishnamoorthy, TIFR, Mumbai for permitting to use the CD spectrometer and time-resolved fluorescence facility, respectively. Urvashi thanks UGC, Govt. of India, for a research fellowship.

References

1. Sharon N (1993) Lectin-carbohydrate complexes of plants and animals: an atomic view. Trends Biochem Sci 18:221–226
2. Wright LM, Van Damme EJM, Barre A, Allen AK, Van Leuven F, Reynolds CD, Rouge P, Peumans WJ (1999) Isolation, characterization, molecular cloning and molecular modelling of two lectins of different specificities from bluebell (*Scilla campanulata*) bulbs. Biochem J 340:299–308
3. Guzman-Partida AM, Robles-Burgueno MR, Ortega-Nieblas M, Vazquez-Moreno I (2004) Purification and characterization of complex carbohydrate specific isolectins from wild legume seeds: *Acacia constricta* is (vinorama) highly homologous to *Phaseolus vulgaris* lectins. Biochimie 86:335–342
4. Singh J, Kamboj SS (2004) A novel mitogenic and anti-proliferative lectin from a wild cobra lily, *Arisaema flavum*. Biochem Biophys Res Commun 318:1057–1065
5. Wright LM, Reynolds CD, Rizkallah PJ, Allen AK, Van Damme EJM, Donovan MJ, Peumans WJ (2000) Structural characterisation of the native fetuin-binding protein *Scilla campanulata* agglutinin: a novel two-domain lectin. FEBS Lett 468:19–22
6. Van Damme EJM, Goossens K, Smeets K, Van Leuven F, Erhaert P, Peumans WJ (1995) The major tuber storage protein of araceae species is a lectin. Characterization and molecular cloning of the lectin from *Arum maculatum*, L. Plant Physiol 107:1147–1158
7. Wright LM, Wood SD, Reynolds CD, Rizkallah PJ, Peumans WJ, Van Damme EJM (1996) Purification, crystallization and preliminary X-ray analysis of a mannose-binding lectin from bluebell (Scilla campanulata) bulbs. Acta Crystallogr D52:1021–1023
8. Van Damme EJM, Allen AK, Peumans WJ (1988) Related mannose-specific lectins from different species of the family Amaryllidaceae. Physiol Plant 73:52–57
9. Peumans WJ, Kellens JT, Allen AK, Van Damme EJM (1991) Isolation and characterize, ation of a seed lectin from elderberry (Sambucus nigra L.) and its relationship to the bark lectins. Carbohydr Res 213:7–17
10. Shangary S, Jatinder S, Sukhdev SK, Kulwant KK, Rajinder SS (1995) Purification and properties of four monocot lectins from the family Araceae. Phytochemistry 40:449–455
11. Singh J, Kamboj SS, Sandhu RS, Shangary S, Kamboj KK (1993) Purification and characterization of a tuber lectin from *Alocasia indica*. Phytochemistry 33:979–983
12. Katre UV, Gaikwad SM, Bhagyawant SS, Deshpande UD, Khan MI, Suresh CG (2005) Crystallization and preliminary X-ray characterization of a lectin from *Cicer arietinum* (chickpea). Acta Crystallogr F61:141–143
13. Katre UV, Suresh CG, Khan MI, Gaikwad SM (2008) Structure–activity relationship of a hemagglutinin from *Moringa oleifera* seeds. Int J Biol Macromol 42:203–207
14. Dharker PN, Gaikwad SM, Suresh CG, Dhuna V, Khan MI, Singh J, Kamboj SS (2009) Comparative studies of two araceous lectins by steady state and time-resolved fluorescence and CD spectroscopy. J Fluoresc 19:239–248
15. Gurjar MM, Khan MI, Gaikwad SM (1998) α-Galactoside binding lectin from *Artocarpus hirsuta*: characterization of the sugar specificity and the binding site. Biochim Biophys Acta 1381:256–264
16. Lakowicz EM, Weber G (1973) Quenching of protein fluorescence by oxygen. Detection of structural fluctuations in proteins on the nanosecond time scale. Biochemistry 12:4171–4179
17. Turoverov KK, Haitlina SY, Pinaev GP (1976) Ultra-violet fluorescence of actin. Determination of actin content in actin preparations. FEBS Lett 62:4–6
18. Su J-T, Kim S-H, Yan Y-B (2007) Dissecting the pretransitional conformational changes in aminoacylase I thermal denaturation. Biophys J 92:578–587

19. He H-W, Zhang J, Zhou H-M, Yan Y-B (2005) Conformational change in the C-terminal domain is responsible for the initiation of creatine kinase thermal aggregation. Biophys J 89:2650–2658
20. Bushmarina NA, Kuznetsova IM, Biktashev AG, Turoverov KK, Uversky VN (2001) Partially folded conformations in the folding pathway of bovine carbonic anhydrase II: a fluorescence spectroscopic analysis. Chembiochem 2:813–821
21. Wong JH, Wong CCT, Ng TB (2006) Purification and characterization of a galactose-specific lectin with mitogenic activity from pinto beans. Biochim Biophys Acta 1760:808–813
22. Kaur A, Kamboj SS, Singh J, Saxena AK, Dhuna V (2005) Isolation of a novel *N*-acetyl-D-lactosamine specific lectin from *Alocasia cucullata* (Schott.). Biotechnol Lett 27:1815–1820
23. Dhuna V, Bains JS, Kamboj SS, Singh J, Shanmugavel AK Saxena (2005) Purification and characterization of a lectin from *Arisaema tortuosum* Schott having in-vitro anticancer activity against human cancer cell lines. J Biochem Mol Biol 38:526–532
24. Siddiqui MZ, Sharma AK, Kumar S (1996) Solution conformation of tuftsin. Int J Biol Macromol 19:99–102
25. Brahamachari SK, Rapaka RS, Bhatnagar RS, Ananthanarayanan VS (1982) Proline-containing β turns in peptides and proteins.II. Physicochemical studies on tripeptides with the Pro-Gly sequence. Biopolymers 21:1107–1125
26. Lehrer SS, Leavis PC (1978) Solute quenching of protein fluorescence. Methods Enzymol 49:222–236
27. Reddy GB, Srinivas VR, Ahmad N, Surolia A (1999) Molten globule-like state of peanut lectin monomer retains its carbohydrate specificity. J Biol Chem 274:4500–4503
28. Redfield C, Smith RAG, Dobson CM (1994) Structural characterization of a highly ordered molten globule at low pH. Nat Struct Biol 1:23–39